Bond Graph Modeling Procedures for Fault Detection and Isolation of Complex Flow Processes

Philippus J. Feenstra[a], Pieter J. Mosterman[b], Gautam Biswas[c], and Peter C. Breedveld[a]

[a] University of Twente, Faculty of Electrical Engineering,
Control Laboratory, P.O. Box 217, 7500 AE Enschede, Netherlands,
P.J.Feenstra@student.utwente.nl, P.C.Breedveld@el.utwente.nl

[b] Institute of Robotics and Mechatronics,
DLR Oberpfaffenhofen, P.O.Box 1116, D-82230 Wessling, Germany,
Pieter.J.Mosterman@dlr.de

[c]Dept. of Electrical Engineering and Computer Science,
Vanderbilt University, Box 1679 Sta. B, Nashville, TN 37235, USA
Biswas@vuse.vanderbilt.edu

Keywords: fault detection and isolation, thermal-fluid systems, hybrid systems, bond graphs, model-based diagnosis, qualitative reasoning

Abstract

Many models for fault detection and isolation (FDI) will contain multi-port energy storage and flow-dependencies due to convection. Converting these models into qualitative ones leads to ambiguities that can be eliminated by analysis of boundary conditions. In this study the example of an automotive cooling system is used to demonstrate how these issues can be handled. Furthermore, time constants in the models need to correspond to the bandwidth of the data acquisition system. In order to achieve this, parameters leading to irrelevant time constants can be eliminated by assigning relatively small and large parameters to be zero or infinite respectively. However, this may result in (i) discontinuities and (ii) zero order causal paths ("algebraic loops"). Compensation of qualitative effects instead of reversal is shown to be an adequate solution for these problems.

INTRODUCTION

Fault detection and isolation (FDI) methods use models for functional redundancy [1, 3]. However, there is little discussion on the design and development of models for this task (see, e.g., [10]). This paper discusses issues involved in designing models for *qualitative* FDI of physical systems that span multiple (e.g., thermal, hydraulic, and mechanical) domains. Qualitative FDI methods do not require precise numerical models. They are less precise than quantitative methods, but more robust to noise (including model deficiencies) and they may provide computational advantages [7].

Our previous work employed the bond graph modeling paradigm [4, 11] for qualitative FDI implemented in our TRANSCEND FDI architecture [5, 7]. The TRANSCEND system has been successfully tested, e.g., in simulation on a secondary sodium cooling system [7] and on real data collected from an automobile engine testbed [2, 5]. The bond graph models for each of these applications were carefully designed and then translated into a temporal causal graph representation (TCG). In case of two-port energy storage phenomena, the qualitative representation may result in ambiguities. Localized analysis of interacting effects and *a priori* knowledge of boundary conditions makes combined behavior explicit and unambiguous.

This paper summarizes the issues dealt with during the model design of an automobile cooling system for FDI. Criteria for developing a bond graph model for use in TRANSCEND are given and it is explained how the derived TCG representation can be tuned to achieve a better model for diagnosis.

QUALITATIVE DIAGNOSIS

Qualitative methods for system analysis typically suffer from spurious results because (i) insufficient constraints are built into the models and (ii) abstraction in the representations makes it hard to differentiate among phenomena [13]. We address the first problem by utilizing the bond graph formalism [4, 11] that inherently en-

forces conservation of energy and power continuity, and provides a generic parsimonious representation across multiple physical domains. The second problem is addressed by carefully refining the model.

The FDI Algorithms

The designed FDI algorithms operate on a temporal causal graph (TCG), a graph that contains the causal relations between system variables, represented as vertices. The edges represent the system parameters and may include temporal behavior, which allows for a graphical description of explicit differential and algebraic equations. The TCG is derived from a bond graph model in a straightforward manner by applying a causality assignment procedure [12] and tracing the causal paths.

This is illustrated for the bond graph of the simplified hydraulics of an automobile cooling system in Fig. 1. The fluid capacities of the radiator, C_{rad}, and block, C_{block}, are connected by an upper hose with resistance, R_{u-hose}, and a lower hose with resistance, R_{l-hose}, that connects to a pump with constant fluid flow, f_m. Although this model can be simplified to a first order system (derivative causality for both capacities is not possible), we distinguish the two capacitances for it to serve as a base model for the extensive form in the next section. Details of deriving the TCG are presented in [7]. Note that, e.g., the relation between the flow and the pressure for the capacities includes a temporal delay, i.e., dt in $\frac{1}{C_{rad}}dt$ on the edge from f_{10} to e_{10} in Fig. 1(b).

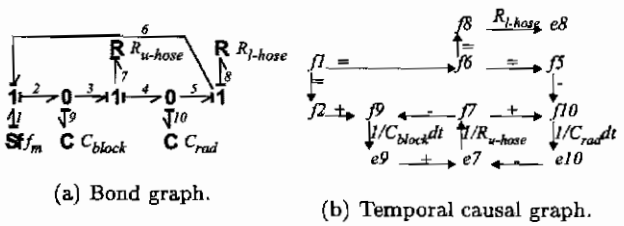

(a) Bond graph.

(b) Temporal causal graph.

Figure 1: Hydraulics of an automobile cooling system.

Given the TCG of the system and a set of one or more deviating measurements, TRANSCEND (i) generates fault hypotheses and (ii) refines these to isolate the true fault. Deviations from nominal behavior are expressed in a qualitative $-$, 0, $+$ form, i.e., below, "around" (e.g. within 5 % of the total range), and above nominal, respectively. These measurements are mapped onto the TCG one-by-one and propagated backward to form the fault hypotheses. For example, if the flow in the upper hose is below its nominal value, i.e., f_7^-, backward propagation implicates the hose resistance as having increased above its nominal value, R_{u-hose}^+, or, tracing further back on the causal path, e_7^-, which implicates C_{block}^+ and C_{rad}^-, and so on. Propagation along a branch terminates when a previously assigned vertex is reached.

Forward propagation in the TCG derives predictions for future behavior for the set of measurements for each hypothesized fault, taking the temporal delays into account. For example, the hypothesized fault R_{u-hose}^+ would cause f_7^-, therefore, f_9^+, and f_{10}^-. Further forward propagation encounters temporal edges, and, therefore, effects on the subsequent vertices are time delayed. This implies that the derivatives for e_9 and e_{10} are affected instead of their magnitudes, indicated by $e_9^{0,+}$. When predictions with a sufficiently high order (a design consideration [8]) are available, propagation terminates. Results for three measurements ($e9$, $e10$ and $f7$) and a flow in the upper hose that is too low, f_7^-, are presented in Fig. 2. These predictions, called *signatures*, are matched with observations on the measurements over time to prune the set of hypothesized faults [7].

derivative order		0^{th}	1^{st}
$R_{u\text{-}hose}^+$	*e9:*	0	+
	e10:	0	−
	f7:	−	+
C_{block}^+	*e9:*	−	+
	e10:	0	−
	f7:	−	+
C_{rad}^-	*e9:*	0	+
	e10:	+	−
	f7:	−	+

Figure 2: Generated hypotheses and their signatures.

The true fault is isolated by using a prediction of its future behavior. However, in some cases the fault parameters are not part of the functional model, e.g., the effect of a leaking hose. Therefore, the failure can be detected but not isolated. In Fig. 1(a), a leakage resistance (i.e., an additional fluid flow path) can be added to one of the 0-junctions. Now the leakage fault can be included in the fault hypotheses set, its future behavior can be predicted, and a leaking pipe fault isolated.

AUTOMOTIVE COOLING SYSTEM MODEL

Karnopp *et al* [4] introduced pseudo bonds, that have convected energy, $\dot{E}_h$, and the temperature T, as variables in the thermal domain and mass flow, $\dot{m}$, and pressure, p, in the hydraulic domain. In this paper, the volume flow, $f_m(= \dot{V})$, is used instead of the mass flow.

Under the assumption that the fluid is incompressible this is the preferred flow variable, and it allows modeling the hydraulic domain with true bonds, which reduces susceptibility to modeling errors (e.g., those that may be caused by the need for additional transformers and gyrators). The measured pressure and temperature variables can be directly linked to the model variables in this approach.

Bond Graph of the Cooling System

The two main thermal storage compartments in the automobile cooling system are: (i) the block and (ii) the radiator, each assumed to be filled with an incompressible cooling fluid, and some air with a constant mass that acts as an ideal gas, see Fig. 3. We assume that the air and fluid do not mix nor does any phase transition take place, so conduction phenomena define their heat interaction.

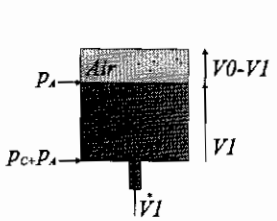

(a) Storage element.

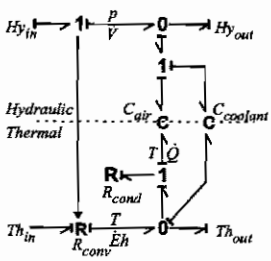

(b) Bond graph.

Figure 3: Storage element and the bond graph of an incompressible cooling fluid and compressible air.

In the bond graph model in Fig. 3(b) only heat, $\dot{Q}$, enters the air capacitance on the thermal side because the mass, m_0, of the air is constant. The constitutive relations are

$$p = \frac{RU}{Vc_v}, \quad T = \frac{U}{m_0 c_v}$$

R is the gas constant, U is the internal energy, V is the volume, c_v is the specific heat at constant volume, and m_0 is the mass. Note that the volume flow of the air is opposite to the volume flow of the coolant, i.e., $\dot{V}_{air} = -\dot{V}_{coolant}$ and that $\dot{V}_{air}$ is a function of the geometry, and $\dot{V}_{coolant}$ is governed by the change of fluid mass. The constitutive relations of the incompressible fluid are

$$p = \frac{V}{A}\rho g, \quad T = \frac{U}{\rho V c}$$

where ρ is the density, A an area, g the gravitational acceleration, and c the specific heat. Because the fluid is incompressible, the mechanical work $\int pdV$ is 0. Therefore, the internal energy U of the coolant becomes $U = U_0 + \int dE_h$. $\dot{E}_h$ is determined by the convection resistance, R_{conv} [4]. The convection energy, $\dot{E}_h = T_u \rho c \dot{V}$, where T_u is the upstream temperature.

The complete model is shown in Fig. 4. The energy storage of air and coolant in the block (and the radiator) is represented by the two capacities C_{blockA} and C_{blockC} (C_{radA} and C_{radC}). The conduction resistance between these is modeled by $R_{blockcond}$ ($R_{radcond}$). The model contains a closed hydraulic power loop at the top and a closed thermal power loop at the bottom. The flow source f_m controls the volume flow, assumed to be constant. The hydraulic resistance of the upper and lower radiator hose is represented by R_{u-hose} and R_{l-hose}, respectively. f_c is the heat from the combustion process. The resistance R_{rad} conducts heat from the radiator to the ambient temperature, T_{amb}. The lower hose leak is represented by resistance R_{leak} and the energy lost is taken into account by the convection resistance R_{conv3}. Conduction of heat by the fluids is assumed negligible in comparison to the heat transferred by convection.

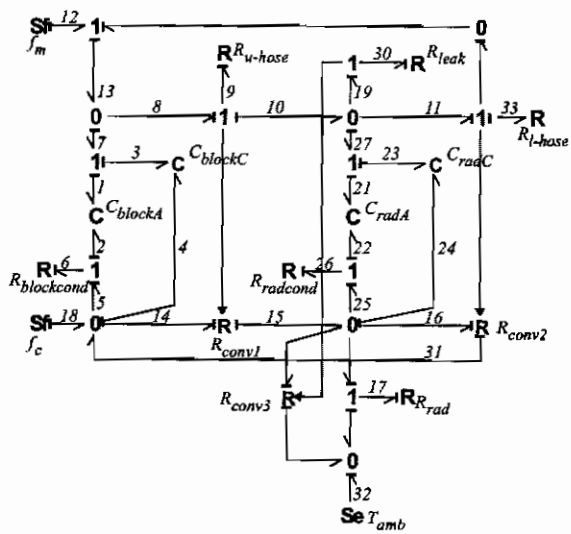

Figure 4: The complete cooling system model.

ADDITIONAL ASSUMPTIONS TO ELIMINATE AMBIGUITIES

To perform FDI with TRANSCEND a qualitative model needs to be generated from the bond graph model given

in the previous section. Due to the use of a multi-port storage and convection, ambiguities can occur. These are eliminated by imposing additional assumptions on the boundary conditions.

The qualitative approach to modeling suffers from reduced discriminatory ability because of the high level of abstraction used in describing variable and parameter values. For example, in Fig. 5(a) the mass and corresponding energy of a storage element, C_C, that contains an incompressible fluid, can be varied by the convection resistance, R_{conv}. The systematically generated TCG is shown in Fig. 5(b). From f_m there are two paths to T with the same order of temporal delay but with opposite sign which causes qualitative reasoning schemes to produce unknown deviations.

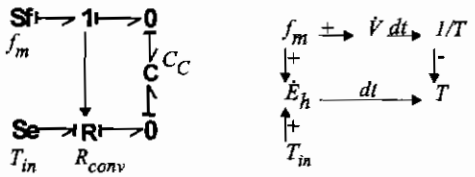

(a) Bond graph. (b) TCG.

Figure 5: Two paths with the same number of temporal delays and opposite sign.

To solve this, the relations of the system, described above, can be directly derived from the bond graph

$$T = \frac{U_0 + \int \dot{U} dt}{\rho c(V_0 + \int f_m dt)} = \frac{U_0 + \int \dot{E}_h dt}{\rho c(V_0 + \int f_m dt)}. \quad (1)$$

If $f_m \leq 0$, the upstream temperature of the convection resistor equals the temperature of the storage element, T, the relation of the temperature becomes

$$T = \frac{U_0 + \rho c \int f_m T dt}{\rho c(V_0 + \int f_m dt)}. \quad (2)$$

The solution of this relation is $T(t) = T_0$, which means that temperature of the capacitance does not change if mass and corresponding energy leave the system. In the situation where $f_m > 0$ and $T_{in} > T$ the temperature relation becomes

$$T = \frac{U_0 + \rho c \int f_m T_{in} dt}{\rho c(V_0 + \int f_m dt)}, \quad (3)$$

where the upstream temperature is T_{in}. Equation (3) and the boundary conditions show that T increases if $f_m > 0$ and $T_{in} > T$. Given this, an unambiguous temporal causal graph can be designed for this subsystem as shown in Fig. 6.

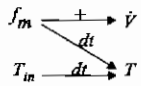

Figure 6: The unambiguous temporal causal graph of Fig. 5, with boundary conditions $T_{in} > T$ and $f_m > 0$.

The same pattern is used to derive the overall unambiguous TCG for the cooling system in Fig. 4, where the radiator and the block are treated as two separate subsystems. The boundary conditions are: $T_{block} > T_{rad} > T_{amb}$ and $f_9 > 0$ and $f_{12} > 0$. In addition, experimental data showed that the influence of the air capacities in the thermal domain could be neglected because of the convected energy. The resulting TCG of the automotive cooling system is presented in Fig. 7.

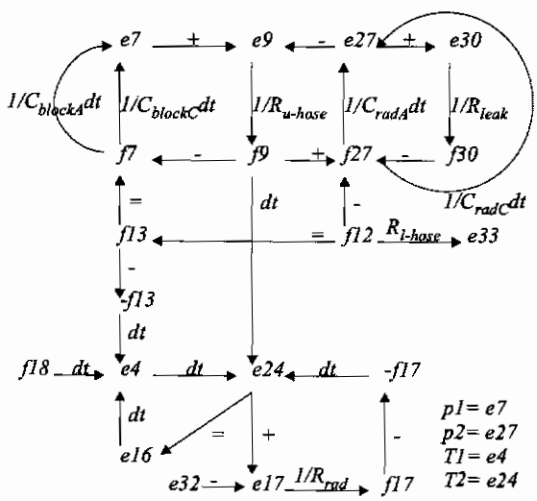

Figure 7: TCG of the automotive cooling system.

HYBRID MODELS

To model a large hose puncture, we may need to consider a very small value for the leakage resistance. In that case, the corresponding dynamic pressure transient may be outside the bandwidth of the data acquisition system, and, therefore, the measured value would show a discontinuity at the point of failure. Figure 8 illustrates this for pressure and temperature measurements with the leak occurring at $t = 5s$. The mismatch between the model

prediction and the observation causes the FDI algorithms to fail in isolating the true fault.

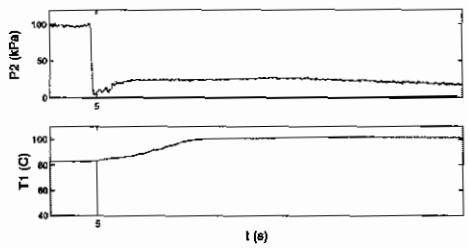

Figure 8: Measured behaviour of the large leak.

This can be resolved by using a *hybrid* model that combines continuous and discrete behavior and operates in a number of distinctive *modes*. In these models, the causality relation between variables may change from one mode to another, and, therefore, a different TCG has to be used for each mode. To model this in the bond graph, a *controlled junction* [6] can be used that switches from *off* to *on* when the fault occurs. Because of this switch, the pressure in the cooling system becomes directly dependent on the ambient pressure, which causes a discontinuous pressure drop.

In general, the use of a different TCG for each mode is computationally intractable. This problem is avoided here by keeping the number of mode changes small. When a fault is detected multiple TCGs corresponding to the different fault hypotheses are generated dynamically and analyzed in parallel. The TCG corresponding to an abrupt leak with the modifications derived above to remove ambiguity is shown in Fig. 9. The abrupt leak result in a causal change that produces a zero order causal path between the C_{radA} and C_{radC}. One of the two capacities has to be set to its derivative causality mode (it acts as a differentiator instead of an integrator). This is marked with a $C_{radA}ddt$ on the corresponding edge of the TCG. Now, a C_{radC} deviation propagated around the loop would return an opposite value of the same order because of the negative gain. Therefore, all deviations would become unknown. This is circumvented by using an algebraic loop algorithm [9] that recognizes that this is a compensating but not reversing effect. In other words, a + deviation is still + but the effect of the + is diminished because of compensation, but not reversed. Also, *ddt* edges imply that there may be impulsive behavior at the time of switching. This is not discussed any further in this paper.

A valve inserted in the lower radiator hose allows controlled insertion of a leakage fault (see Fig. 8). The failure is detected and backward propagation generates the fault hypotheses R^-_{leak}, C^+_{blockA}, C^+_{blockC}, C^+_{radA}, C^+_{radC}, R^-_{u-hose} and R^+_{rad}.

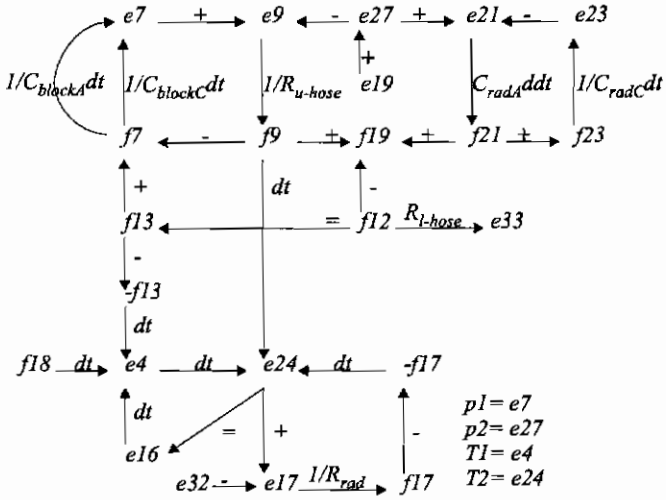

Figure 9: TCG for leakage fault.

step 0

		actual			
	p_2:	−	.	*	.
	T_1:	+	.	.	.
R^-_{leak} (fast)	p_2:	−	.	.	.
	T_1:	0	0	+	−
R^-_{leak} (slow)	p_2:	0	−	+	−
	T_1:	0	0	0	+
C^+_{blockA}	p_2:	0	+	−	+
	T_1:	0	0	−	+
C^+_{blockC}	p_2:	0	+	−	+
	T_1:	0	0	−	+
C^+_{radA}	p_2:	−	+	−	+
	T_1:	0	0	+	−
C^+_{radC}	p_2:	−	+	−	+
	T_1:	0	0	+	−
R^-_{u-hose}	p_2:	0	+	−	+
	T_1:	0	0	+	−
R^+_{rad}	p_2:	0	0	0	0
	T_1:	0	0	+	−

step 1

		actual			
	p_2:	−	0	.	.
	T_1:	+	+	.	.
R^-_{leak} (fast)	p_2:	−	.	.	.
	T_1:	0	0	+	−
C^+_{radA}	p_2:	−	+	−	+
	T_1:	0	0	+	−
C^+_{radC}	p_2:	−	+	−	+
	T_1:	0	0	+	−

Figure 10: The signatures of the fault hypothesis

Forward propagation derives the signatures of the fault hypotheses that are compared with the real measurements in the refinement step. Measurements are represented in the form $p_2^{+,-,*}$, where the * denotes an abrupt deviation. Here 2^{nd} and higher order derivations are not calculated from the measurements. The information derived from the measurements eliminates five of the eight fault hypotheses (see Fig. 10). Lack of discriminatory evidence provided by the two measurements allows no further refinement. The set of three final fault hypotheses is accurate because $R^-_{leak}(fast)$ is included.

CONCLUSIONS

This paper describes the application of our qualitative FDI approach to a thermal-fluid system: the cooling system of an automobile engine. We develop a pseudo bond graph model of the system and demonstrate the FDI effectiveness with real data collected from our automotive test bed. A number of new and interesting issues have been dealt with in this paper.

The interaction between the thermal and hydraulic power domains, modeled as two-port storage elements, causes double paths with opposite sign in the TCG representation that we use for fault hypothesis generation and refinement. To avoid ambiguities that do not permit further analysis, we describe an additional procedure using boundary value assumptions to determine unambiguous causal relations for a two-port energy storage element.

Hybrid models handle the mismatch between the model order and the bandwidth of the data acquisition system, but, unless the mode identification problem can be solved in general, this approach can lead to computational intractability during FDI analysis. We are now conducting further studies on efficient hybrid diagnosis and on methods to resolve the ambiguity of algebraic loops in qualitative FDI analysis.

References

[1] R. Clark, P. Frank, and R. Patton. Introduction. In *Fault Diagnosis in Dynamic Systems: Theory and Applications*, chapter 1, pages 1–19. Prentice-Hall, UK, 1989.

[2] P. J. Feenstra, E. J. Manders, P. J. Mosterman, G. Biswas, and J. Barnett. Modeling and instrumentation for fault detection and isolation of a cooling system. In *Proceedings of the IEEE Southeastern Conference 2000*, pages 365–372, Nashville, TN, Apr. 2000.

[3] R. Isermann. A review on detection and diagnosis illustrate that process faults can be detected when based on the estimation of unmeasurable process parameters and state variables. *Automatica: IFAC Journal*, 20(4):387–404, 1989.

[4] D. Karnopp, D. Margolis, and R. Rosenberg. *Systems Dynamics: A Unified Approach.* John Wiley and Sons, New York, 2 edition, 1990.

[5] E. J. Manders, P. J. Mosterman, and G. Biswas. Signal to Symbol Transformation Techniques for Robust Diagnosis in TRANSCEND. In *Tenth International Workshop on Principles of Diagnosis*, pages 155–165, Lock Awe Hotel, Scotland, June 1999.

[6] P. J. Mosterman and G. Biswas. A theory of discontinuities in dynamic physical systems. *Journal of the Franklin Institute*, 335B(3):401–439, Jan. 1998.

[7] P. J. Mosterman and G. Biswas. Diagnosis of continuous valued systems in transient operating regions. *IEEE Transactions on Systems, Man, and Cybernetics*, 29(6):554–565, Nov. 1999.

[8] P. J. Mosterman, G. Biswas, and N. Sriram. Measurement Selection and Diagnosability of Complex Dynamic Systems. In *Eighth International Workshop on Principles of Diagnosis*, pages 79–86, Mont St. Michel, France, Sept. 1997.

[9] P. J. Mosterman, E. J. Manders, and G. Biswas. Qualitative Dynamic Behavior of Physical System Models With Algebraic Loops. In *International Workshop on Principles of Diagnosis.* pages 155–162, Morelia, Mexico, 2000.

[10] B. Ould Bouamama, F. Busson, G. Dauphin-Tanguy, and M. Staroswiecki. Analysis of structural properties of thermodynamic systems. In *Safeprocees, 4th IFAC Symposium on Fault Detection Supervision and Safety for Technical Processes*, volume 2, pages 1068–1073, Budapest, June 2000.

[11] H. M. Paynter. *Analysis and Design of Engineering Systems.* The M.I.T. Press, Cambridge, Massachusetts, 1961.

[12] J. van Dijk. *On the role of bond graph causality in modelling mechatronic systems.* PhD dissertation, University of Twente, Den Haag, The Netherlands, 1994. ISBN 90-9006903-8.

[13] D. Weld and J. de Kleer. *Readings in Qualitative Reasoning about Physical Systems.* Morgan Kaufmann, San Mateo, CA, 1990.